https://doi.org/10.5194/egusphere-2025-4610
Preprint. Discussion started: 17 March 2026

Methane Emissions Estimation from China's Leading Coal Production Hub: A Hybrid Hyperspectral Satellite Observations and Emission Inventory Framework

Authors: Shengxi Bai[1,2,3], Huilin Chen[2,4], Zhen Zhang[5], Shushi Peng[6], Fei Jiang[1,2,3], Fei Li[1,2], Shuzhuang Feng[1,2], Yingqi Yan[1,2], Qidan Huang[1,2], Yongguang Zhang[1,2,3]*

Affiliations:

[1]International Institute for Earth System Sciences, Jiangsu Center for Collaborative Innovation in Geographical Information Resource Development and Application, Nanjing University, Nanjing, Jiangsu 210023, China.

[2]Frontiers Science Center for Critical Earth Material Cycling, Nanjing University, Nanjing, Jiangsu 210023, China.

[3]Jiangsu International Joint Carbon Neutrality Laboratory, Nanjing, Jiangsu, 210023, China.

[4]Joint International Research Laboratory of Atmospheric and Earth System Sciences, School of Atmospheric Sciences, Nanjing University, Nanjing, China

[5]Institute of Tibetan Plateau Research , Chinese Academy of Science, Beijing, China

[6]College of Urban and Environmental Sciences, Peiking Univeristy, Beijing, China

Corresponding author: Yongguang Zhang (ygz@nju.edu.cn)

https://doi.org/10.5194/egusphere-2025-4610
Preprint. Discussion started: 17 March 2026

Abstract

Accurate estimation of coal mine methane (CMM) emissions in Shanxi Province, China's leading coal production hub, is essential for mitigating China's anthropogenic methane emissions. Hyperspectral remote sensing is an emerging method for real-time methane monitoring with significant potential for optimizing CMM emission factors. However, limited satellite revisit frequencies can introduce biases in CMM emission estimates. To address these issues, we developed a Hierarchical Bayesian Inversion Algorithm utilizing time-series observations from seven hyperspectral satellites in Shanxi (2019-2023), comprising 215 methane plumes from 26 coal mines, to estimate annual CMM emission rates with limited satellite revisit frequency. Subsequently, we integrated multi-source satellite observations with inventory data to estimate CMM emissions in Shanxi province. Our analysis yields a CMM emission factor of $(7.9 \pm 1.4)\times10^{-3}$ Tg/Mt for Shanxi, with CMM emissions reaching 11 ± 2 Tg/yr in 2023. We demonstrate that CMM emissions follow a right-skewed distribution in Shanxi Province, where low-frequency extreme methane emission events (≥10000 kg/h) constitute approximately 25% of all time-series observations. Additionally, our results reveal that capacity reduction policies initially decreased CMM emissions, but subsequent production recovery led to emission increases, with asymmetric responses to coal price fluctuations. Our findings establish a novel strategy for CMM accounting from hyperspectral satellite observations.

Keywords: Coal mine methane emission, Hyperspectral satellite, Bayesian Inversion, Annual emission estimates, Emission factor optimization

https://doi.org/10.5194/egusphere-2025-4610
Preprint. Discussion started: 17 March 2026

1 Introduction

China is the world's largest coal producer, with coal mine methane (CMM) emissions representing the dominant anthropogenic methane source (bp, n.d.; Liu et al., 2021; Peng et al., 2016; Saunois et al., 2020). Mitigating Chinese CMM emissions is critical for climate change mitigation. Shanxi Province, China's leading coal production hub, accounts for ~15% of global coal production (Peng et al., 2023) and ~21% of China's CMM emissions (Yue et al., 2012). Prioritizing the assessment and control of methane emissions from major coal production hubs represents an effective strategy for reducing China's overall CMM emissions (Lu et al., 2021), requiring reliable emission assessment data for guidance.

Bottom-up emission inventories provide spatially extensive, long-term estimates of Chinese CMM emissions using standardized national and regional emission factors (Commission et al., 2023; Scarpelli et al., 2022). However, with the advancement of China's coal industry reforms and rapid technological development, these standardized emission factors increasingly diverge from observed CMM emission levels (Gao et al., 2021; Kang et al., 2024; Khanna et al., 2024; Wang et al., 2024a). Although recent studies have developed bottom-up corrections for Chinese CMM emissions (Chen et al., 2024; Zhang et al., 2023), the spatiotemporal variability of CMM emissions makes it challenging for bottom-up emission factors to accurately characterize emission patterns (Tibrewal et al., 2024). Consequently, existing bottom-up estimates for Chinese and Shanxi CMM emissions remain inconsistent with ground-based and satellite monitoring observations (Guo et al., 2023; Miller et al., 2019).

Top-down methods assimilating satellite and ground data through atmospheric transport models reveal spatiotemporal emission characteristics while improving estimation accuracy (Chen et al., 2022; Miller et al., 2019; Zhang et al., 2022). The TROPOspheric Monitoring Instrument (TROPOMI) can observe atmospheric methane column enhancements at 7 km × 3.5 km spatial resolution, providing 0.1° × 0.1° resolution estimates of Shanxi CMM emissions through Bayesian inversion (Peng et al., 2023). While these top-down approaches offer sufficient spatial resolution to identify significant CMM emission regions, they face limitations in attributing methane column enhancements to specific mines when developing targeted mitigation measures, particularly in coal-dense production hubs (Hong et al., 2021; Lauvaux et al., 2022; Schuit et al., 2023; Tan et al., 2023).

Hyperspectral satellites can accurately identify coal mine point sources at high spatial resolution (Han et al., 2024; He et al., 2024). However, due to cloud cover and revisit frequency, hyperspectral satellite observations of methane emissions from individual mines are limited and prone to capturing extreme emission events (Bai et al., 2024; Han et al., 2024; He et al., 2024; Qin et al., 2024). This leads to biased estimates of annual methane emission based on limited hyperspectral satellite observations—a challenge that extends to anthropogenic methane monitoring from oil/gas facilities and landfills (Beaven and Scheutz, 2019; Irakulis-Loitxate et al., 2024). The limited revisit frequency of hyperspectral satellites, which hampers characterization of significant temporal emission variability, represents a widely recognized barrier requiring urgent resolution.

To address these research gaps, this study utilized observations from seven hyperspectral satellites (GF5-01, GF5-02, ZY1-02D/02E, PRISMA, GHGSat, EnMAP, EMIT) overpassing Shanxi Province during 2019-2023 to develop a novel Hierarchical Bayesian inversion algorithm for accurately estimating annual methane emission flux rates from coal mines with low satellite

https://doi.org/10.5194/egusphere-2025-4610
Preprint. Discussion started: 17 March 2026

revisit frequencies. Integrating top-down satellite observations with bottom-up inventory data, we calculated the CMM emission factor for Shanxi, established a facility-level inventory, and analyzed temporal characteristics of Shanxi CMM emissions from 2000-2023. Our findings provides an optimization strategy for national/regional CMM accounting.

2 Data and Methods

2.1 Datasets

We analyzed images from seven hyperspectral satellites (GF5-01, GF5-02, ZY1-02D/02E, PRISMA, GHGSat, EnMAP, EMIT) overpassing Shanxi Province during 2019-2023 to estimate CMM emissions. Mines with ⩾3 satellite revisits were classified as having time-series methane observations, with extracted data forming the Shanxi CMM emission time-series dataset. **Figure A1** shows the temporal distribution of effective methane plume detections from seven hyperspectral satellites for these mines. Mines with <3 revisits were classified as having limited observations, with missing data in at least two seasons.

The Global Coal Mine Tracker (GCMT) is an open-source database that records detailed information on representative surface and underground coal mines globally (Global Energy Monitor, 2023). The database encompasses key parameters including annual production (Mt), mine size (km^2), mine depth (m), workforce size, coordinates, and operational status. While GCMT exhibits spatial gaps in documenting small-medium coal mines in Shanxi Province due to restricted access to government websites and limited availability of physical documentation, its high degree of open accessibility facilitates global application of methodologies developed using this database. The representative coal mine dynamics captured in GCMT effectively reflect regional spatiotemporal characteristics of coal mining activities, making it a preferred data source for validation and comparative assessment in existing CMM emission accounting studies (Bai et al., 2024; Han et al., 2024; Hauenstein, 2023; Jasansky et al., 2023; Sadavarte et al., 2022; Scarpelli et al., 2025). Consequently, we coupled the GCMT database with observations from seven hyperspectral satellites to calculate CMM emission factors for Shanxi Province and establish a facility-level methane emission inventory.

Due to incomplete coverage of mines in GCMT, we used Berkeley Lab's annual Shanxi coal production statistics (2000-2023) (Lin et al., 2025) for provincial emission calculations. Monthly coal prices (Qinhuangdao Q5500 thermal coal and Australia Newcastle steam coal spot prices) were averaged annually to analyze economic influences on emission trends (Wang et al., 2024b).

2.2 Methane plume detection and quantification from hyperspectral satellites

We employed Matched Filter algorithm to retrieval the methane column enhancements from six satellites (Bai et al., 2024; Dennison et al., 2013; Foote et al., 2020; Thompson et al., 2015) (GHGSat data products provided pre-processed results). GEOS-FP 10-m wind data (U_{10}) were used to support manual plume identification; a plume was deemed valid when its elongation direction formed an acute angle with the wind vector (**Figure A2a–c**) (Lauvaux et al., 2022). Plume origins were attributed to specific coal mines using Google Earth imagery, and high-value pixels within each plume were assigned to the corresponding emission facility (**Figure A2d**). In this case, all three plumes traced back to ventilation shafts at the same mine. Methane flux rates were estimated using the Integrated Mass Enhancement (IME) method

https://doi.org/10.5194/egusphere-2025-4610
Preprint. Discussion started: 17 March 2026

(Frankenberg et al., 2016; Irakulis-Loitxate et al., 2024), with effective wind speed (U_{eff}) relationships derived from large eddy simulations conducted in Changzhi, Shanxi (Fei et al., 2023).

Controlled methane release experiments have comprehensively validated the precision of methane point-source emission detection and quantification using multiple hyperspectral satellites (Sherwin et al., 2023). Quantification uncertainties remain consistently minimal across all satellite platforms and research teams (Sherwin et al., 2024). For all emissions identified through hyperspectral measurements, the parity plots from each satellite team demonstrate strong concordance with the theoretical 1:1 relationship. Mean estimation accuracy exceeds 80% for all satellite team combinations, while R^2 values for linear regression of fully blinded assessments range between 0.89 and 0.97 (Li et al., 2024; Sherwin et al., 2023, 2024). These validation results confirm the robust capability of hyperspectral satellite platforms to identify and quantify methane point-source emissions through Matched Filter and IME methodologies.

We attributed 26 mines with time-series observations linked to 215 methane plumes. Among GCMT-recorded mines with detected emissions (n=13), seven had time-series observations and six had limited observations from hyperspectral satellites.

2.3 Hierarchical Bayesian Inversion Algorithm

To accurately estimate annual methane fluxes and reduce estimation errors caused by limited hyperspectral satellite revisit frequencies, we developed a novel Hierarchical Bayesian inversion algorithm. The algorithm extracts global and seasonal characteristics from 2019-2023 Shanxi time-series observations, combining these with limited target mine observations to estimate annual methane emission fluxes, as illustrated in **Figure 1**.

Prior Characteristic Extraction: Global prior characteristics $Q \sim Lognormal(\mu_0, \sigma_0^2)$ and seasonal prior characteristics $Q|S \sim Lognormal(\mu_{s,0}, \sigma_{S,0}^2)$ were extracted from the 2019-2023 Shanxi Province coal mine time-series hyperspectral satellite methane emission observation dataset.

First-Layer Bayesian Update: The global prior characteristics undergo first-layer Bayesian updating using limited methane emission observations from the target mine to generate global posterior characteristics $Q|X \sim Lognormal(\mu_{post}, \sigma_{post}^2)$, which characterize the target mine's overall emission tendency.

Second-Layer Bayesian Update: For seasons with target mine methane emission observations, the seasonal prior characteristics are updated through second-layer Bayesian updating using the target mine's hyperspectral satellite methane emission observations for that season, generating seasonal posterior characteristics $Q|S, x_S \sim Lognormal(\mu_{s,post}, \sigma_{S,post}^2)$ and inversely estimating seasonal methane emission flux rates. For seasons lacking target mine methane emission observations, the target mine's global posterior characteristics serve as indirect information for second-layer Bayesian updating of seasonal prior characteristics, generating seasonal posterior characteristics $Q|S', x_{S'} \sim Lognormal(\mu_{s',post}, \sigma_{S',post}^2)$ and inversely estimating methane emission flux rates for missing observation seasons.

Annual Flux Estimation: Annual methane emission flux rates for target mines with limited observations are obtained by averaging the hierarchical Bayesian inversion results across all four seasons.

https://doi.org/10.5194/egusphere-2025-4610
Preprint. Discussion started: 17 March 2026

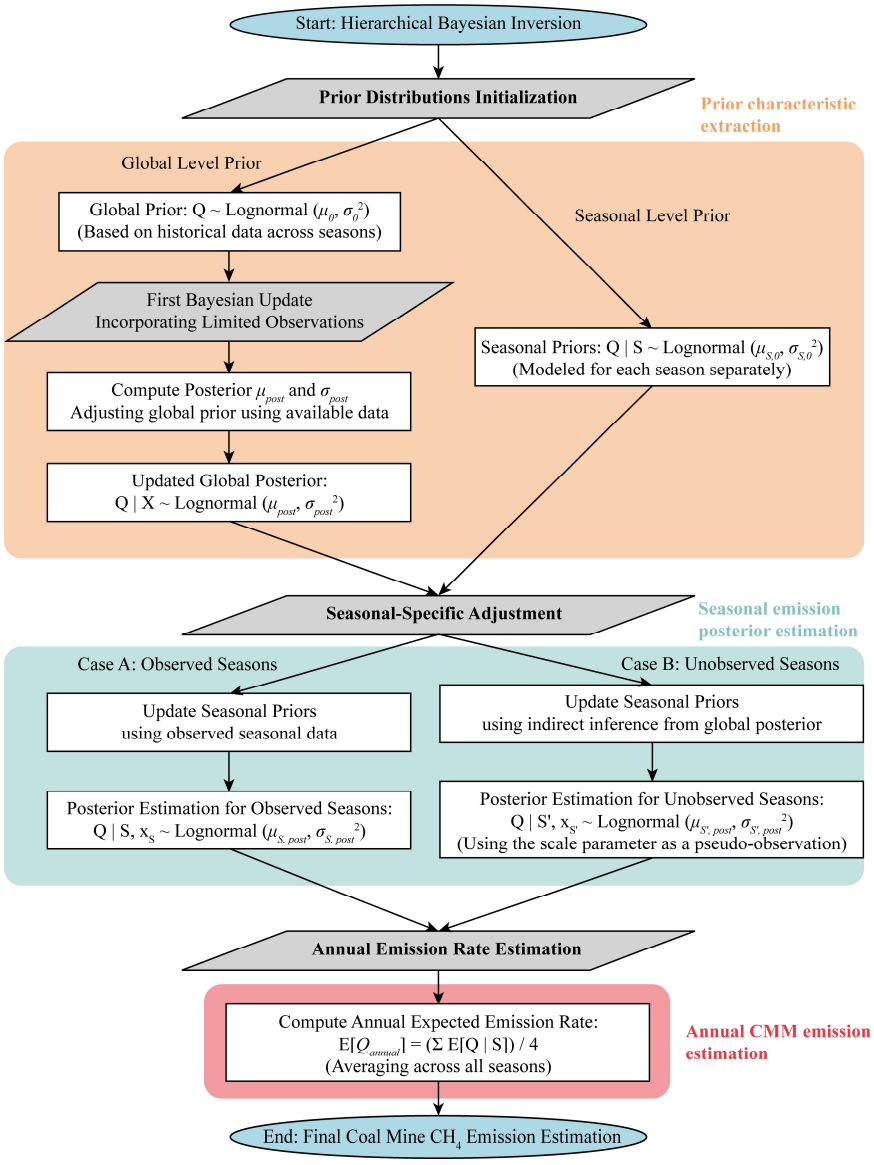

Figure 1. Hierarchical Bayesian Inversion Algorithm framework: (1) extraction of prior characteristics from hyperspectral satellite observations (orange box), (2) posterior estimation of seasonal emissions for coal mines with limited observations (cyan box), and (3) calculation of annual methane emissions (red box).

https://doi.org/10.5194/egusphere-2025-4610
Preprint. Discussion started: 17 March 2026

2.4 Coal mine methane emission factor

This study integrates top-down observations from seven hyperspectral satellites with coal mine attribute information from the GCMT database to calculate the Shanxi CMM emission factor (EF, Tg/Mt). Despite limitations posed by cloud cover and revisit frequency constraints of hyperspectral satellite observations, as well as incomplete coal mine records in the GCMT database, we successfully identified 13 operational coal mines that were consistently detected by both satellite observations and documented in the GCMT database. These 13 coal mines are geographically distributed across western Xinzhou, southern Yangquan, northern Jinzhong, and central Changzhi regions of Shanxi Province—areas where TROPOMI has detected significant methane column concentration enhancements and which encompass typical coal mining districts (Peng et al., 2023).

Consequently, We derived the Shanxi CMM EF by calculating the coal production-weighted average of EFs from these 13 representative coal mines that were both observed by hyperspectral satellites for methane emissions and recorded in the GCMT database, as shown in **Eq.(1)** (Chen et al., 2024; Lin et al., 2025):

$$EF = \frac{Q_1}{Prod_1} \times \frac{Prod_1}{\sum_{i=1}^{13} Prod_i} + \cdots + \frac{Q_{13}}{Prod_{13}} \times \frac{Prod_{13}}{\sum_{i=1}^{13} Prod_i} = \frac{\bar{Q}}{\overline{Prod}} \tag{1}$$

where Q_i and $\bar{Q}$ represent the methane emission flux rate of each individual coal mine and the mean methane emission flux rate of the 13 coal mines, respectively (Tg/yr). For the seven coal mines with time-series methane emission observations, Q_i values correspond to the temporal mean of their respective time-series observations. For the six coal mines with limited methane emission observations, Q_i values were estimated using the established Hierarchical Bayesian inversion algorithm. $Prod_i$ and $\overline{Prod}$ represent the annual coal production of each individual mine and the mean annual coal production of the 13 coal mines, respectively (Mt/yr). The $Prod_i$ values for each mine were obtained from the GCMT database.

Following uncertainty propagation principles, we calculated the uncertainty (σ_{EF}, Tg/Mt) of the EF using **Eq.(2)**, Here, σ_{Q_i} represents the uncertainty in methane emission flux rate for each coal mine. For mines with time-series methane emission observations, we calculated σ_{Q_i} using **Eq.(3)-(6)**:

$$\sigma_{EF} = \left|\frac{\partial_{EF}}{\partial_{\bar{Q}}}\right| \cdot \sigma_{\bar{Q}} = \frac{1}{\overline{Prod}} \cdot \sigma_{\bar{Q}} = \frac{\sum_{i=1}^{13} \sigma_{Q_i}}{13 \cdot \overline{Prod}} \tag{2}$$

$$\sigma_{Q_i} = \frac{1}{N} \sum_{i=1}^{N} \sigma_{q_i} \tag{3}$$

$$\sigma_{q_i} = q \times \frac{\sigma_{U_{eff}}}{U_{eff}} \times 2 \tag{4}$$

$$\sigma_{U_{eff}} = \sigma_{U_{10}} \times 0.37^2 \tag{5}$$

https://doi.org/10.5194/egusphere-2025-4610
Preprint. Discussion started: 17 March 2026

$$\sigma_{U_{10}} = -\frac{1}{6600}\tau + 2.55 \quad (6)$$

where N represents the number of satellite revisits to the coal mine by the seven hyperspectral satellites, and σ_{q_i} represents the uncertainty in methane emission rate (q) estimates when hyperspectral satellites overpass the coal mine. Following the approach of Li et al. (2023), we implemented identical assumptions to derive the computational framework in **Eq.(4)** (Varon et al., 2018). The uncertainty quantification for U_{eff} in **Eq.(5)** was established through linear regression analysis of the U_{eff}-U_{10} relationship parameterized via large eddy simulation modeling (Li et al., 2023). Based on GEOS-FP U_{10} uncertainties ($\sigma_{U_{10}}$) reported by Veron et al. (2018), we developed the relationship expressed in **Eq.(6)** to characterize $\sigma_{U_{10}}$ as a function of plume lifetime (τ).

We calculated σ_{Q_i} for coal mines with limited methane emission observations through random sampling inversion estimation experiments. First, we constructed scenarios with limited methane emission observations (one or two observations) using time-series observations from Gucheng coal mine in Shanxi Province. Gucheng mine had 18 hyperspectral satellite time-series observations spanning four seasons from 2019-2023, making it representative. From the 18 time-series observations at Gucheng mine, we randomly selected 1 observation 10 times and 2 observations 15 times, ensuring these 25 random samples were non-overlapping, thereby creating 25 scenarios of Gucheng mine with limited methane emission observations. Second, we applied the established Hierarchical Bayesian inversion algorithm to estimate CMM emission flux rates for these 25 limited observation scenarios, with results shown in **Figure A3**. We found that methane emission flux rates estimated from two observations were closer to the mean of Gucheng mine's 18 time-series observations (reference value, $\bar{y}$) than those estimated from single observations, indicating that higher satellite revisit frequencies capture more information related to CMM emission patterns. Finally, we calculated σ_{Q_i} for coal mines with limited observations using **Eq.(7)**, based on the methane emission flux rate ($\hat{y}_i$) estimates from the 25 (k value) simulation scenarios.

$$\sigma_{Q_i} = \sqrt{\frac{1}{k}\sum_{i=1}^{k}(\hat{y}_i - \bar{y})^2} \quad (7)$$

A facility-level CMM emission inventory for Shanxi Province was established by applying the Shanxi CMM EF to annual production data for each coal mine in the GCMT dataset. Provincial-level emissions for 2000-2023 were estimated by multiplying the Shanxi CMM EF by Berkeley Lab's annual coal production statistics for Shanxi Province, as detailed in **Section 2.1**.

https://doi.org/10.5194/egusphere-2025-4610
Preprint. Discussion started: 17 March 2026

3 Results and discussion

3.1 Point-source methane emission intensities from coal mines in Shanxi Province

Hyperspectral satellites provide precise detection of methane enhancement plumes from coal mine emissions at fine spatial resolution. **Figure 2** illustrates representative examples of methane plumes captured by seven hyperspectral satellite platforms in Shanxi Province. Our analysis reveals substantial variability in emission rates across CMM plumes. Notably, GF5-01 detected a methane plume from a coal mine in Changzhi during winter 2019 with an emission rate of $(5.9 \pm 2.5)\times10^3$ kg/h, approximately twice the emission rate observed by EnMAP at the same facility during winter 2022. However, both observations were significantly lower than the emission rate captured by PRISMA during winter 2021, which recorded $(1.1 \pm 0.5)\times10^4$ kg/h at the identical coal mine. Similarly, GF5-02 detected a methane plume from this coal mine in May 2022, approximately one-third of the emission rate observed by GHGSat at the same facility in June of the same year. In contrast to the Changzhi coal mine with time-series hyperspectral satellite observations, EMIT captured only a single methane emission event from a coal mine in Xinzhou during winter 2023, recording an emission rate of $(9.8 \pm 3.5)\times10^3$ kg/h. This observation approaches the emission rate detected by PRISMA at the Changzhi coal mine during the same seasonal period in 2021, yet remains significantly higher than other methane plume examples from the Changzhi facility presented in **Figure 2**.

Our hyperspectral satellite observations of CMM emissions in Shanxi Province reveal pronounced temporal variability in emission characteristics. Accurate quantification of CMM emissions necessitates time-series observational data to characterize temporal emission patterns, including seasonal variations, for reliable annual methane emission estimates. However, the revisit frequency of current hyperspectral satellites is constrained by operational parameters and atmospheric conditions such as cloud cover, resulting in preferential detection of extreme methane emission events rather than systematic monitoring of emission patterns. This limitation is exemplified by EMIT's single extreme emission observation from the Xinzhou coal mine (**Figure 2**). Consequently, annual methane emission estimates based solely on limited observational records would introduce substantial estimation biases. Therefore, establishing comprehensive time-series hyperspectral satellite observation databases through multi-satellite collaborative monitoring represents a critical step toward addressing this challenge. By leveraging time-series hyperspectral satellite observations of CMM emissions, we can extract characteristic emission patterns to improve the accuracy of annual methane emission accounting for coal mines with limited observational coverage.

https://doi.org/10.5194/egusphere-2025-4610
Preprint. Discussion started: 17 March 2026

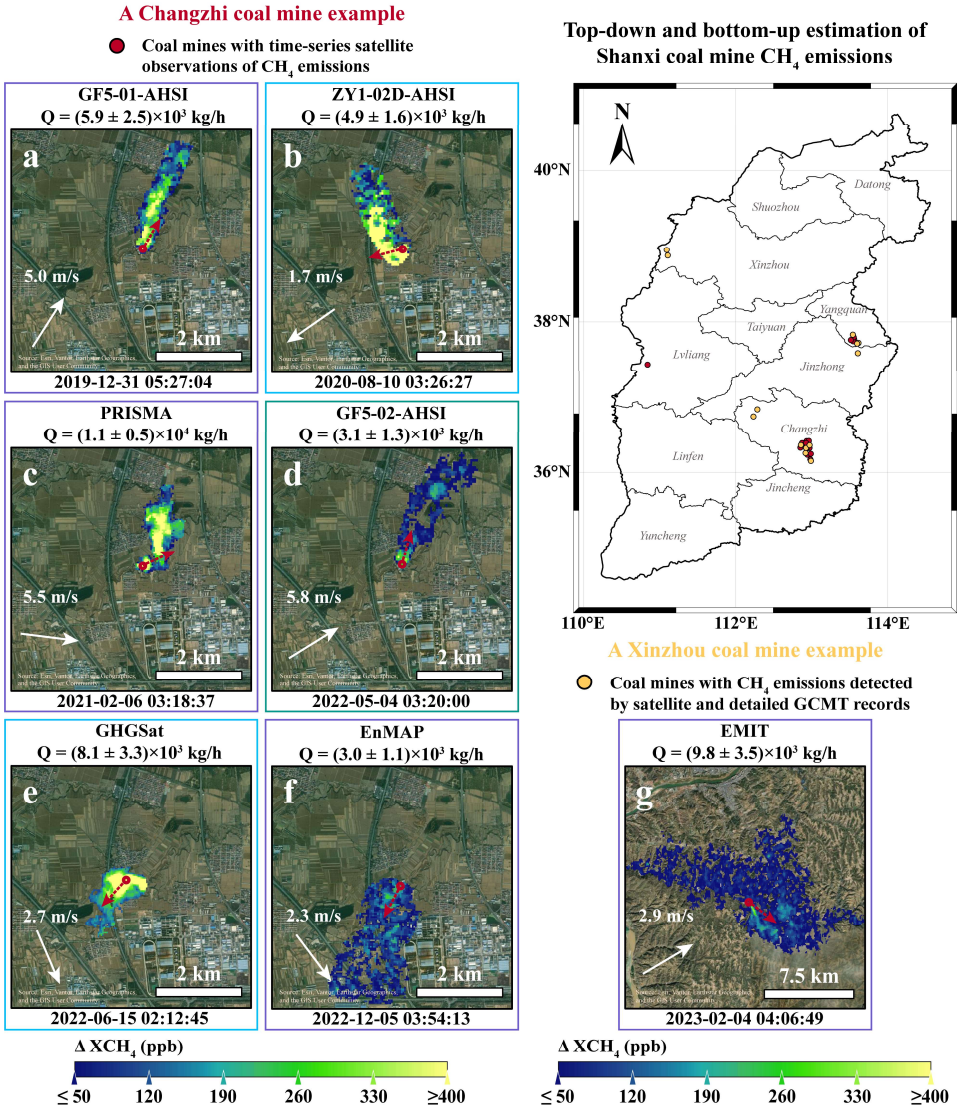

Figure 2. Hyperspectral satellite methane plume detection and quantification results: (a)-(f) Examples of methane plume masks from GF5-01, ZY1-02D, PRISMA, GF5-02, GHGSat, and EnMAP for a coal mine in Changzhi with time-series observations; (g) EMIT methane plume mask for a coal mine in Xinzhou. The red dashed arrow denotes the methane concentration gradient direction near the plume source. The upper-right inset shows spatial distribution of coal mines with time-series hyperspectral satellite methane observations and GCMT-recorded mines with detected emissions in Shanxi. Background RGB imagery in (a)-(g) is Powered by Esri.

https://doi.org/10.5194/egusphere-2025-4610
Preprint. Discussion started: 17 March 2026

3.2 Coal mine methane emission factors in Shanxi Province

We employed our Hierarchical Bayesian Inversion Algorithm to optimize annual average methane emission rates for 6 coal mines with limited hyperspectral satellite observations from 13 GCMT-recorded mines with detected emissions. Coupling hyperspectral satellite observations with GCMT inventory data yielded a CMM emission factor of $(7.9 \pm 1.4)\times10^{-3}$ Tg/Mt for Shanxi Province.

Accurate estimation of annual methane emissions requires comprehensive understanding of coal mine emission patterns. **Figures 3a** and **3b** demonstrate that emission rates from 26 coal mines with time-series hyperspectral observations exhibited predominantly right-skewed distributions, as did emission rates from 215 observed methane plumes. This heavy-tailed distribution characterizes temporal variability in CMM emissions through extreme events that substantially exceed typical levels. These infrequent extreme events, typically exceeding 10000 kg/h, constitute approximately 25% of all time-series observations (**Figure 3b**). Seasonal distributions also exhibit right-skewness (**Figures A4**), with autumn (shape=0.98) and winter (shape=0.92) demonstrating the most pronounced skewness. The time-series observations reveal significant seasonal differences in CMM emissions (Kruskal-Wallis test, $H=17.29$, $p<0.001$). To assess whether uneven observation frequency across seasons affects this seasonal pattern, we conducted bootstrap resampling by randomly subsampling autumn and winter observations to match the minimum seasonal sample size ($n=18$). Across 1000 iterations, 100% of tests yielded significant seasonal differences ($p<0.05$, **Figure A5**), confirming that the observed seasonal emission characteristics are robust and independent of sampling frequency disparities.

Figure 3c presents hyperspectral satellite observations from 6 coal mines with limited data availability. Baode mine exhibited only one extreme winter emission event. Given the right-skewed characteristics of coal mine emissions, direct extrapolation of annual emissions from this single observation would result in significant overestimation. Our Hierarchical Bayesian Inversion Algorithm integrated this observation with global and seasonal characteristics derived from time-series data, producing an optimized annual average emission rate 46% lower than the extreme winter observation. Yuwu and Sijiazhuang mines each possessed two observations, both containing one extreme event exceeding 10000 kg/h. Since such extreme events occur infrequently within the right-skewed distribution framework, calculation of annual emissions from the arithmetic mean of two observations would overestimate emissions by artificially amplifying extreme event frequency. Our algorithm effectively integrated satellite observations with captured emission pattern characteristics, thereby optimizing annual average estimates for Yuwu and Sijiazhuang mines to values 29% and 32% below their respective observation means. Notably, annual production and methane emissions should theoretically demonstrate strong positive correlation (Liu et al., 2024). **Figure A6** reveals that the Pearson correlation coefficient between our algorithm's emission estimates and annual production (0.78) exceeds that between satellite observations and production, indicating effective reduction of bias introduced by extreme emission values.

We compared our satellite-inventory coupled CMM emission factor for Shanxi Province with existing bottom-up estimates (**Figure 3d**). Berkeley Laboratory assumed a fixed provincial emission factor to calculate historical emissions, deriving $(6.6 \pm 1.1)\times10^{-3}$ Tg/Mt from 2011 National Mine Safety Administration data—lower than our $(7.9 \pm 1.4)\times10^{-3}$ Tg/Mt estimate (Lin

https://doi.org/10.5194/egusphere-2025-4610
Preprint. Discussion started: 17 March 2026

et al., 2025). Chen et al. (2024) used the same 2011 data but considered China's 2010-2019 coal industry capacity reduction plan involving gradual mine closures. Though tracking all abandoned mines during this period remains challenging, Chen et al. estimated annual emission factors accounting for closure policy impacts. Their 2010-2019 estimates cluster around 8.7×10^{-3} Tg/Mt, closely approximating our results. Zhang et al. (2023) extrapolated 2016-2023 annual factors from 2019 measurements at 182 Shanxi mines, yielding a mean of 6.44×10^{-3} Tg/Mt, similar to Berkeley's estimates but lower than our estimation.

The aforementioned bottom-up studies employed identical methods to calculate methane emission factors for individual coal mines: measuring absolute methane emission quantities on designated days within specific months under government guidance, then calculating ratios with corresponding daily production (Zhang et al., 2023). This approach facilitates large-scale surveys of CMM emission conditions. However, CMM emissions exhibit significant right-skewed characteristics, making this method inadequate for capturing temporal variability in CMM emissions, particularly prone to overlooking extreme methane emission events, potentially resulting in underestimation. In deriving the CMM emission factor for Shanxi Province, our study extracted methane emission characteristics from five years of time-series hyperspectral satellite methane emission observations, specifically considering right-skewed properties caused by extreme methane emission events. This may explain why our estimated CMM emission factor for Shanxi Province exceeds those of Berkeley Laboratory (Lin et al., 2025) and Zhang et al (2023). In contrast, our derived CMM emission factor for Shanxi Province closely approximates Chen et al. (2024)'s results, possibly because Chen et al. considered the Chinese government's coal industry capacity reduction plan, providing a more realistic representation of actual CMM emission scenarios in Shanxi Province at the provincial level (Gao et al., 2021).

https://doi.org/10.5194/egusphere-2025-4610
Preprint. Discussion started: 17 March 2026

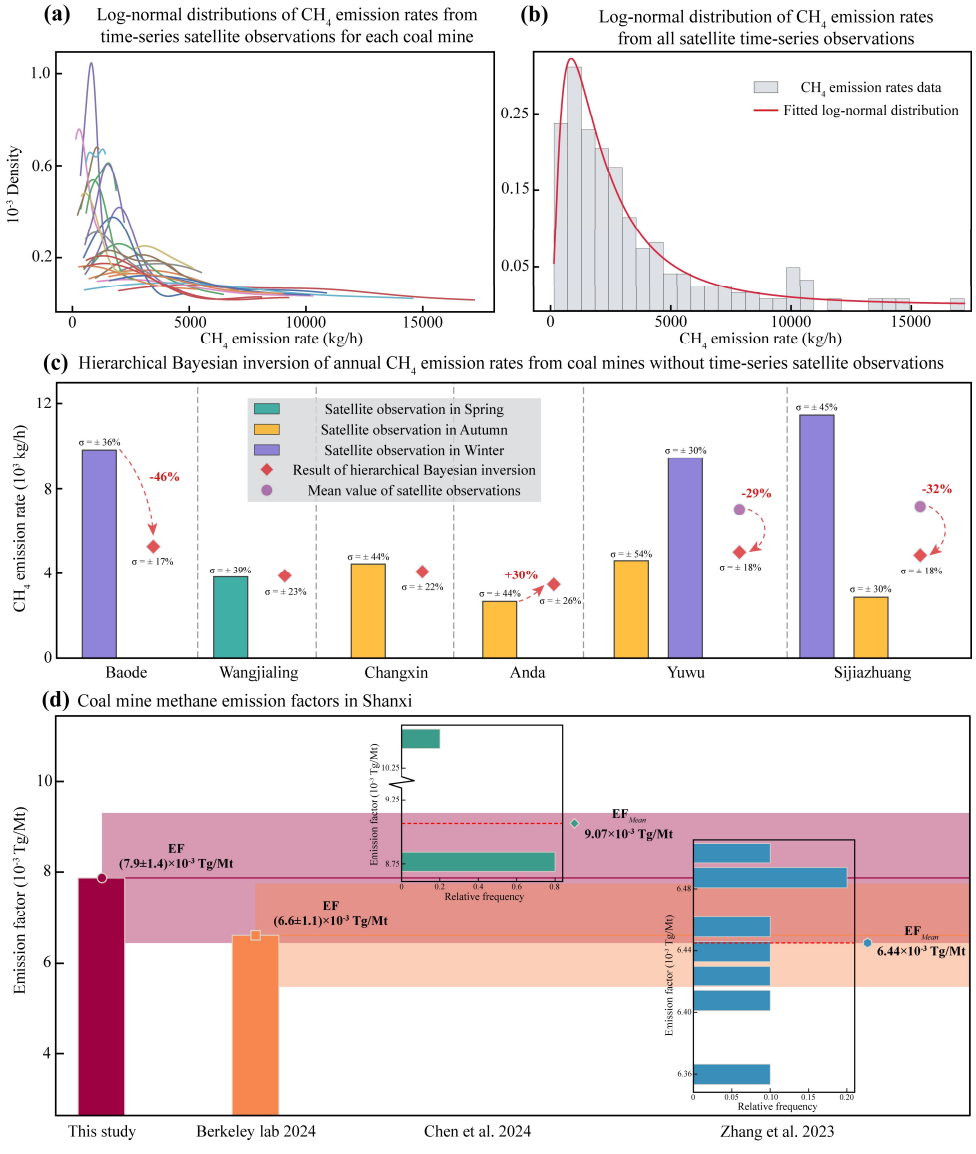

Figure 3. (a)-(b) Emission rate distributions for coal mines with time-series observations; (c) Annual emission estimates using Hierarchical Bayesian Inversion Algorithm for mines with limited satellite revisits. The σ shows the uncertainty in satellite observations and hierarchical Bayesian inversion results; (d) Comparison of coal mine methane emission factors.

https://doi.org/10.5194/egusphere-2025-4610
Preprint. Discussion started: 17 March 2026

3.3 Spatiotemporal characteristics of regional coal mine methane emissions in Shanxi Province

Our analysis reveals that Shanxi Province's CMM emissions reached 11 ± 2 Tg/yr in 2023. **Figure 4a** illustrates the spatial distribution of CMM emissions across Shanxi Province. Coal production regions in Yangquan, Changzhi, and central Jincheng exhibited dense mine distributions, corresponding to primary methane column concentration enhancement zones observed by TROPOMI (Peng et al., 2023). Prefecture-level analysis revealed strong positive correlations between methane emissions and operational characteristics (**Figures 4b, 4c**). Total annual methane emissions correlated strongly with maximum mining depth ($r = 0.72$, $p < 0.05$), reflecting increased coalbed gas pressure and methane content at greater depths (Langmuir, 1918). A significant positive correlation also existed with total mine size ($r = 0.60$, $p < 0.05$), indicating the influence of production scale. However, mining depth exerted a more pronounced influence on methane emissions than mine area.

The temporal characteristics of CMM emissions in Shanxi from 2000-2023 are illustrated in **Figure 4d**. Emissions increased continuously from 2000-2008, followed by a reduction in 2009 coinciding with the implementation of the Eleventh Five-Year Plan for Coal Industry Development (Yang et al., 2024), which aimed to optimize coal distribution, regulate total production, and consolidate small- and medium-sized mines. However, China's coal-dominated energy structure drove a renewed rapid increase in emissions from 2010 onwards. Following large-scale energy transition and air pollution control measures implemented by the Chinese government in 2013, emissions began declining in 2015. The expansion of coal production led to a gradual increase in emissions from 2017, reaching 11 ± 2 Tg/yr in 2023. While the Berkeley Laboratory (Lin et al., 2025), Sheng et al. (2019), and Zhang et al. (2023) bottom-up assessments show consistent temporal trends with our study, their estimated annual emission intensities are consistently lower. Chen et al. (2024) demonstrated fluctuating declining trends for 2011-2015, differing from other studies, though their post-2015 trends align with previous research and their annual emission intensities approximate our estimates. Peng et al. (2023)'s top-down TROPOMI-based estimate for 2019 yielded 8.5 ± 0.6 Tg/yr, exceeding both our integrated estimate of 7.6 ± 1.4 Tg/yr and Chen et al. (2024)'s bottom-up estimate of 7.56 Tg/yr. For 2020, Peng et al. (2023)'s top-down estimate of 8.6 ± 0.6 Tg/yr closely matches our integrated estimate of 8.4 ± 1.5 Tg/yr and Chen et al. (2024)'s bottom-up estimate of 8.74 Tg/yr. Notably, methane emissions from open-pit mines fall below the detection limits of both TROPOMI and the hyperspectral satellites, potentially biasing satellite-derived provincial emission estimates scaled by production.

To elucidate the economic drivers underlying the gradual decline followed by steady increase in emissions during 2008-2022, we further conducted correlation analyses between CMM emissions and coal prices (**Figure 4e**). Both our estimates and those from Berkeley Laboratory (Lin et al., 2025) demonstrate significant positive correlations between time-series emissions and domestic QHD coal prices as well as international NEWC coal prices for 2008-2022. This relationship likely reflects China's domestic coal supply dominance (Guo et al., 2025), with Shanxi serving as the leading coal production hub. Rising coal prices stimulate provincial production and consequently increase methane emissions, while declining prices reduce mining enterprise profitability, potentially affecting production and emissions. Following brief price increases and subsequent sustained declines from 2009-2016, Sheng et al. (2019)'s emission estimates did not immediately decrease but rather decelerated growth before declining four years later, consistent with our findings and those of Berkeley Laboratory (Lin et al., 2025).

https://doi.org/10.5194/egusphere-2025-4610
Preprint. Discussion started: 17 March 2026

Chen et al. (2024)'s estimates during this period exhibited "decline-increase-decline" fluctuations following price drops, with significant reductions occurring four years later. These patterns indicate that while price declines can diminish coal production incentives, China's coal-dominated energy structure and sustained high demand prevent immediate emission reductions following price decreases. Post-2016 price increases correspond with rising emission trends across all studies examined.

https://doi.org/10.5194/egusphere-2025-4610
Preprint. Discussion started: 17 March 2026

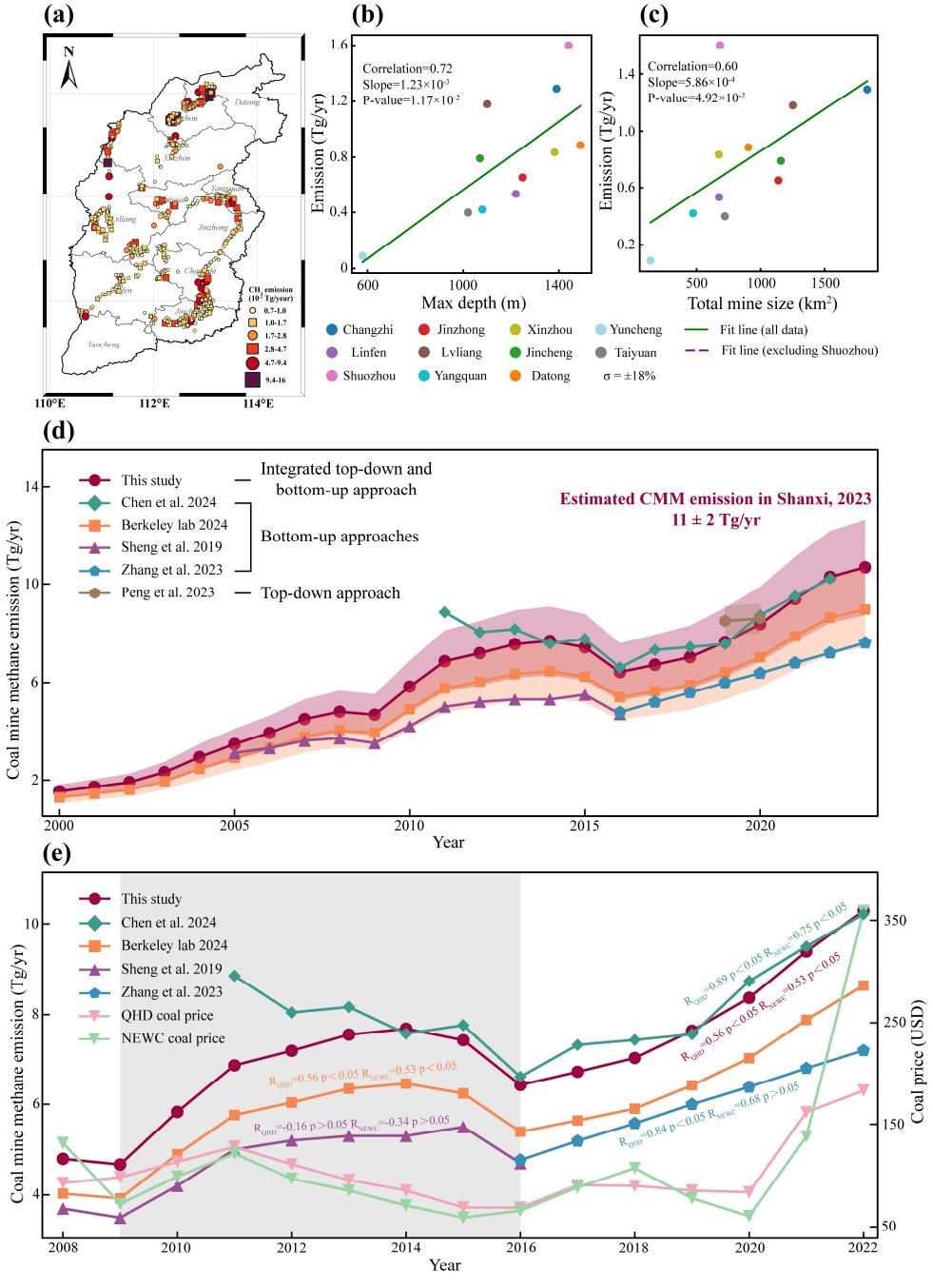

398

https://doi.org/10.5194/egusphere-2025-4610
Preprint. Discussion started: 17 March 2026

Figure 4. Spatiotemporal characteristics of Shanxi coal mine methane emissions: (a) Annual methane emission fluxes and spatial distributions for 526 coal mines in 2023; (b) Prefecture-level correlations between total annual methane emission and maximum mining depth; (c) Prefecture-level correlations between total annual methane emission and total mine size. The σ shows the uncertainty in prefecture-level coal mine methane emission estimates; (d) Time-series methane emissions (2000-2023) from bottom-up, top-down, and integrated approaches. The shaded area adjacent to the line plot represents the estimated uncertainty range; (e) Correlation analysis between QHD coal price (representing China's coal price) and NEWC coal price (representing international coal price) with temporal variations of Shanxi coal mine methane emissions (2008-2022).

4 Conclusions

Accurate quantification of CMM emissions in Shanxi Province, China's leading coal production hub, is essential for national anthropogenic methane accounting. This study demonstrates the potential of integrating multi-hyperspectral satellite observations with inventory data to enhance emission factor derivation at provincial scales. The developed Hierarchical Bayesian Inversion Algorithm addresses a critical limitation in satellite-based methane monitoring—sparse temporal coverage—by leveraging regional emission patterns to constrain annual estimates for individual mines.

Our derived provincial emission factor of $(7.9 \pm 1.4)\times10^{-3}$ Tg/Mt and 2023 emissions of 11 ± 2 Tg/yr for Shanxi Province provide updated constraints for China's methane inventory. The spatial heterogeneity analysis reveals emission hotspots in Yangquan, Changzhi, and central Jincheng, offering targeted guidance for emission reduction prioritization. The identified temporal patterns reflect policy impacts on CMM emission, with asymmetric responses to price fluctuations providing insights into emission drivers.

The framework established here offers significant environmental benefits for global methane monitoring. Notably, the limited revisit frequency of hyperspectral satellites poses a challenge for accurate emission factor estimation, for which coordinated multi-satellite observation provides an effective solution. The 12-satellite GHGSat constellation, for instance, achieves substantially higher revisit frequencies than the GF/ZY series. With the deployment of MethaneSAT and Tanager-1 in 2024 and additional methane-monitoring satellites planned, both the temporal coverage and spatial extent of coal mine point-source observations are expected to increase markedly. Furthermore, recent studies indicate that uncertainty in point-source methane emission estimates is predominantly driven by wind speed and methane column enhancements retrieval uncertainties, the latter propagated through the IME method. Future work will prioritize developing more robust retrieval algorithms to reduce these uncertainties and enhance emission quantification accuracy. Moreover, detection limits inherent to hyperspectral satellites may lead to the underestimation of minor emission sources; integrating satellite observations with ground-based measurements thus offers a pathway toward more responsive and precise anthropogenic methane accounting. This study presents a novel approach for deriving CMM emission factors through coordinated multi-satellite observations—one that is readily scalable to refine CMM emission factors worldwide, thereby improving greenhouse gas inventory accuracy and informing evidence-based climate mitigation strategies.

https://doi.org/10.5194/egusphere-2025-4610
Preprint. Discussion started: 17 March 2026

Appendix

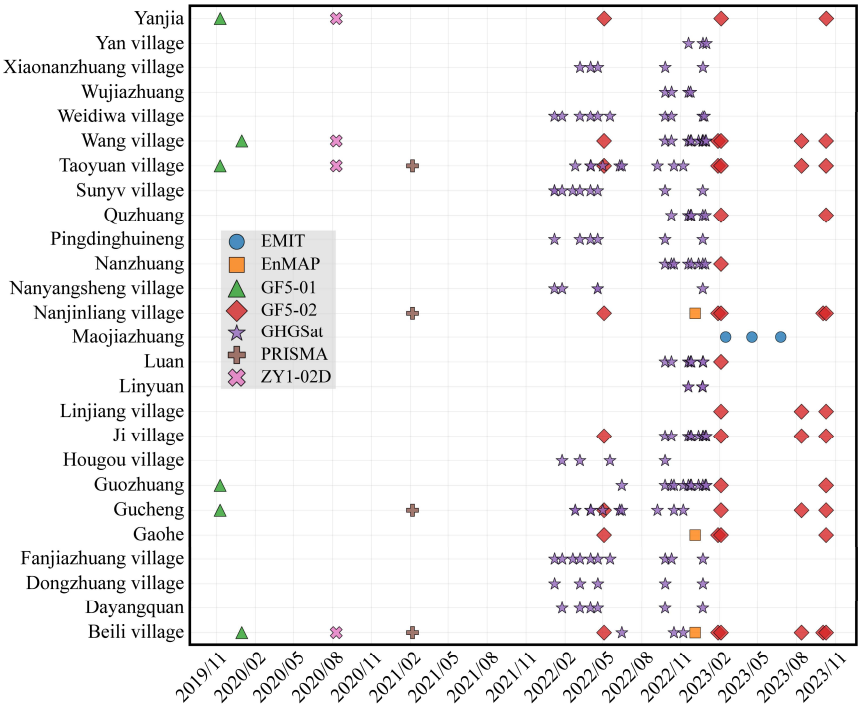

Figure A1. Methane plume detection statistics for mines with time-series observations by hyperspectral satellites: The x-axis represents detection timestamps by seven hyperspectral satellites, and the y-axis represents mines with time-series methane observations.

https://doi.org/10.5194/egusphere-2025-4610
Preprint. Discussion started: 17 March 2026

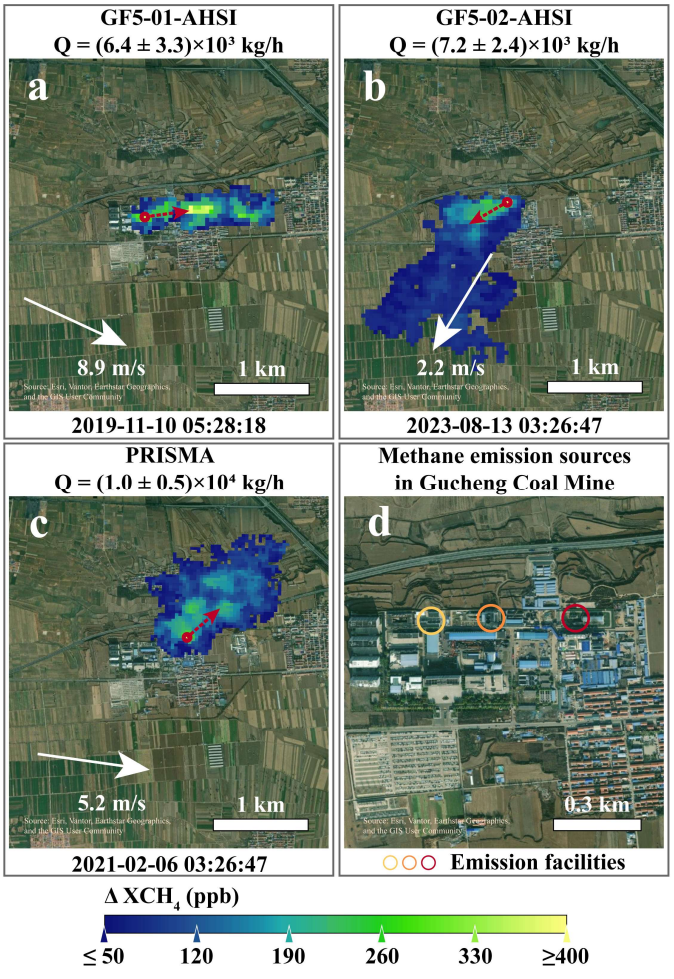

Figure A2. Examples of methane plume identification and source attribution. (a)–(c) Methane plumes observed by GF5-01, GF5-02, and PRISMA, respectively, and attributed to the Gucheng coal mine. (d) Attribution of the three methane plumes to their respective emission sources within the coal mine. The red dashed arrow denotes the methane concentration gradient direction near the plume source. The circled features indicate the attributed facilities. Background RGB imagery in (a)-(d) is Powered by Esri.

https://doi.org/10.5194/egusphere-2025-4610
Preprint. Discussion started: 17 March 2026

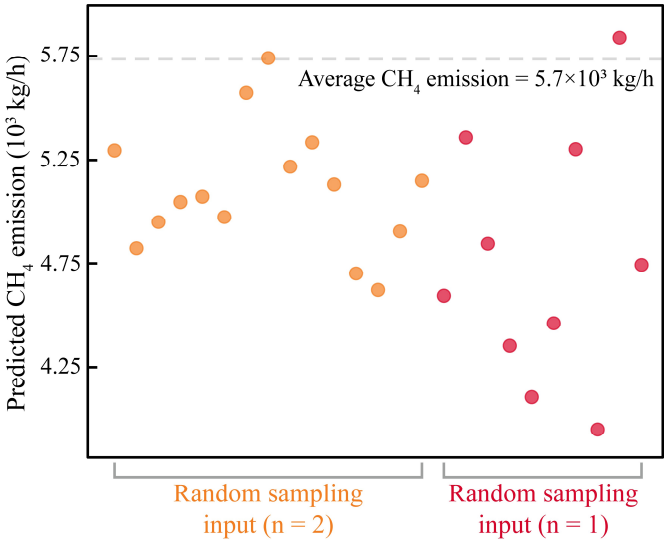

Figure A3. Results of the random sampling inversion estimation experiment.

https://doi.org/10.5194/egusphere-2025-4610
Preprint. Discussion started: 17 March 2026

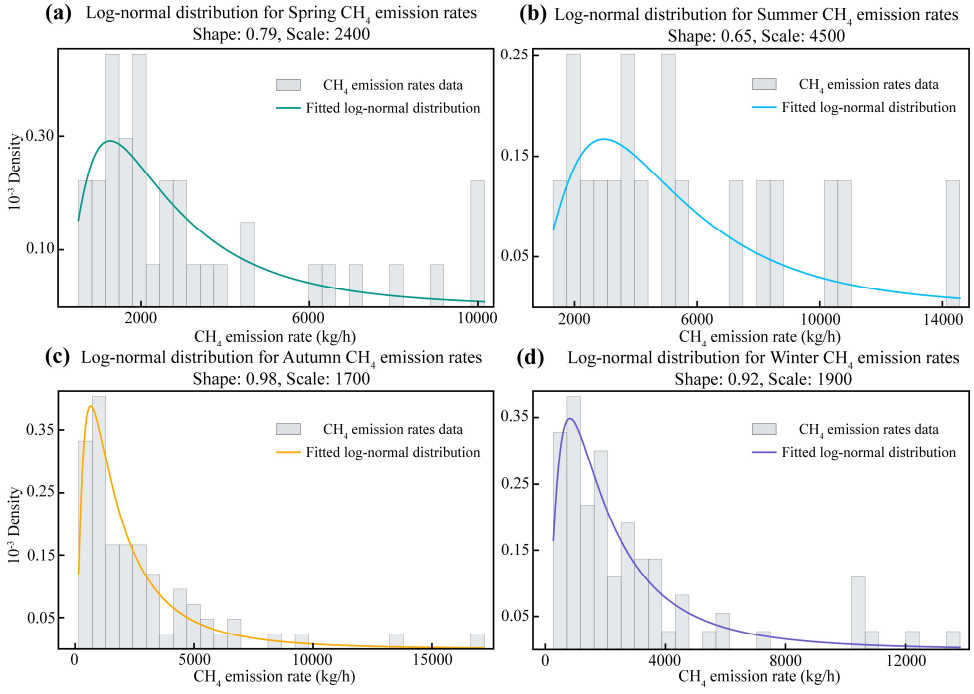

Figure A4. Seasonal characteristics of time-series hyperspectral satellite observations from Shanxi coal mines.

https://doi.org/10.5194/egusphere-2025-4610
Preprint. Discussion started: 17 March 2026

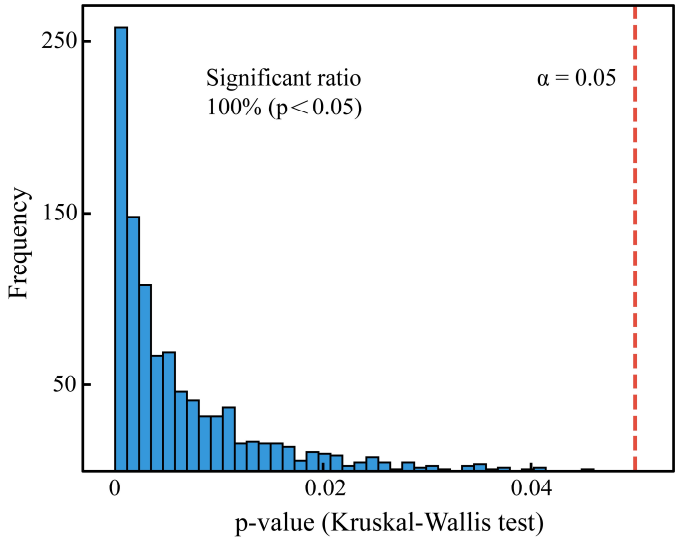

Figure A5. Bootstrap analysis with subsampled autumn-winter observations.

https://doi.org/10.5194/egusphere-2025-4610
Preprint. Discussion started: 17 March 2026

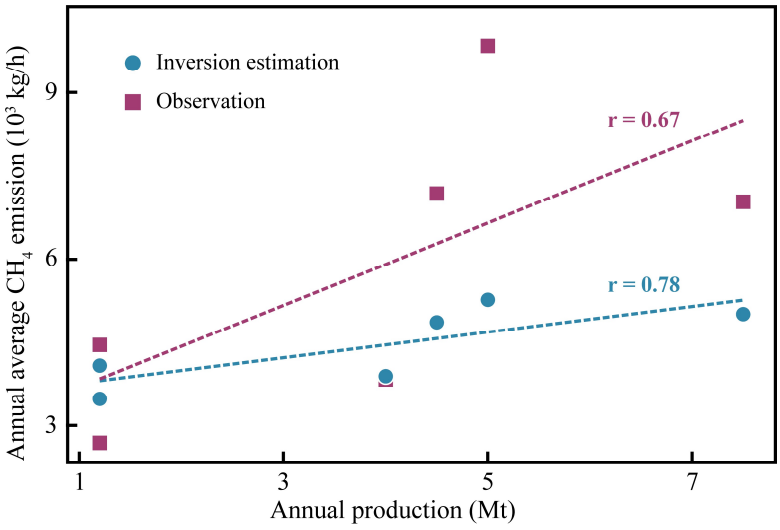

Figure A6. Comparison of annual average methane emissions from coal mines.

https://doi.org/10.5194/egusphere-2025-4610
Preprint. Discussion started: 17 March 2026

Data availability

The Global Coal Mine Tracker data can be downloaded at https://globalenergymonitor.org/. PRISMA data are available at https://prismauserregistration.asi.it/. EMIT data are available at https://search.earthdata.nasa.gov/search. GF5-01, GF5-02, and ZY1-02E data are available at http://114.116.226.59/english/normal/. EnMAP data are available at https://www.enmap.org/data_access/. GHGSat-C1 to C5 data are available at https://www.ghgsat.com/en/products-services/data-sat/.

Author contribution

SB and YZ conceived and designed the research. SB analyzed data, and prepared the paper. HC, ZZ, SP, FJ, FL, SF, YY and QH reviewed and commented on the paper.

Competing interests

At least one of the (co-)authors is a member of the editorial board of Atmospheric Chemistry and Physics.

Acknowledgments

This research was supported by the National Science Foundation of China (U24A20590), the National Key Research and Development Program of China (2022YFE0209100), and the Fundamental Research Funds for the Central Universities - Cemac “GeoX” Interdisciplinary Program (No. 2024300245). We thank for the technical support of the National large Scientific and Technological Infrastructure “Earth System Numerical Simulation Facility”. Our gratitude also extends to China Centre for Resources Satellite Data and Application for the GF5 series and ZY1-02E data. Furthermore, we acknowledge the efforts of Italian Space Agency, NASA's Jet Propulsion Laboratory, GHGSat, Inc., and the German Aerospace Center's Space Agency for sharing the PRISMA, EMIT, GHGSat-C1 to C5, and EnMAP data. Lastly, we would like to acknowledge the anonymous reviewers for their insightful and constructive comments, which aided in improving the quality of our manuscript.

https://doi.org/10.5194/egusphere-2025-4610
Preprint. Discussion started: 17 March 2026

References

Bai, S., Zhang, Y., Li, F., Yan, Y., Chen, H., Feng, S., Jiang, F., Sun, S., Wang, Z., Zhou, C., Zhou, W., and Zhao, S.: High-resolution satellite estimates of coal mine methane emissions from local to regional scales in Shanxi, China, Science of The Total Environment, 950, 175446, https://doi.org/10.1016/j.scitotenv.2024.175446, 2024.

Beaven, R. and Scheutz, C.: Landfill gas emission monitoring, Waste Management, 87, 833–834, https://doi.org/10.1016/j.wasman.2019.02.039, 2019.

bp: Full report – Statistical Review of World Energy 2021, n.d.

Chen, D., Ma, M., Hu, L., Du, Q., Li, B., Yang, Y., Guo, L., Cai, Z., Ji, M., Zhu, R., and Fang, X.: Characteristics of China's coal mine methane emission sources at national and provincial levels, Environ Res, 259, 119549, https://doi.org/10.1016/j.envres.2024.119549, 2024.

Chen, Z., Jacob, D. J., Nesser, H., Sulprizio, M. P., Lorente, A., Varon, D. J., Lu, X., Shen, L., Qu, Z., Penn, E., and Yu, X.: Methane emissions from China: a high-resolution inversion of TROPOMI satellite observations, Atmos Chem Phys, 22, 10809–10826, https://doi.org/10.5194/acp-22-10809-2022, 2022.

Commission, E., Centre, J. R., Crippa, M., Guizzardi, D., Schaaf, E., Monforti-Ferrario, F., Quadrelli, R., Risquez Martin, A., Rossi, S., Vignati, E., Muntean, M., Brandao De Melo, J., Oom, D., Pagani, F., Banja, M., Taghavi-Moharamli, P., Köykkä, J., Grassi, G., Branco, A., and San-Miguel, J.: GHG emissions of all world countries – 2023, Publications Office of the European Union, https://doi.org/doi/10.2760/953322, 2023.

Dennison, P. E., Thorpe, A. K., Roberts, D. A., and Green, R. O.: Modeling sensitivity of imaging spectrometer data to carbon dioxide and methane plumes, in: 2013 5th Workshop on Hyperspectral Image and Signal Processing: Evolution in Remote Sensing (WHISPERS), 1–4, https://doi.org/10.1109/WHISPERS.2013.8080614, 2013.

Fei, L. I., Shiwei, S. U. N., Yongguang, Z., Chenxi, F., Cuihong, C., Huiqin, M. A. O., and Yinnian, L. I. U.: Mapping methane super-emitters in China and United States with GF5-02 hyperspectral imaging spectrometer, National Remote Sensing Bulletin, 1–15, https://doi.org/10.11834/jrs.20232453, 2023.

Foote, M. D., Dennison, P. E., Thorpe, A. K., Thompson, D. R., Jongaramrungruang, S., Frankenberg, C., and Joshi, S. C.: Fast and Accurate Retrieval of Methane Concentration From Imaging Spectrometer Data Using Sparsity Prior, IEEE Transactions on Geoscience and Remote Sensing, 58, 6480–6492, https://doi.org/10.1109/TGRS.2020.2976888, 2020.

Frankenberg, C., Thorpe, A. K., Thompson, D. R., Hulley, G., Kort, E. A., Vance, N., Borchardt, J., Krings, T., Gerilowski, K., Sweeney, C., Conley, S., Bue, B. D., Aubrey, A. D., Hook, S., and Green, R. O.: Airborne methane remote measurements reveal heavy-tail flux distribution in Four Corners region, Proceedings of the National Academy of Sciences, 113, 9734–9739, https://doi.org/10.1073/pnas.1605617113, 2016.

Gao, J., Guan, C., Zhang, B., and Li, K.: Decreasing methane emissions from China's coal mining with rebounded coal production, Environmental Research Letters, 16, 124037, https://doi.org/10.1088/1748-9326/ac38d8, 2021.

Global Energy Monitor: Global Coal Mine Tracker, October 2023.

Guo, J., Gao, J., Yan, K., and Zhang, B.: Unintended mitigation benefits of China's coal de-capacity policies on methane emissions, Energy Policy, 181, 113718, https://doi.org/10.1016/j.enpol.2023.113718, 2023.

Guo, J., Gao, J., Yan, K., Zhang, B., and Liu, H.: Global coal trade induces large CH4 emissions, iScience, 28, 112073, https://doi.org/10.1016/j.isci.2025.112073, 2025.

Han, G., Pei, Z., Shi, T., Mao, H., Li, S., Mao, F., Ma, X., Zhang, X., and Gong, W.: Unveiling Unprecedented Methane Hotspots in China's Leading Coal Production Hub: A Satellite Mapping Revelation, Geophys Res Lett, 51, e2024GL109065, https://doi.org/10.1029/2024GL109065, 2024.

Hauenstein, C.: Stranded assets and early closures in global coal mining under 1.5◦C, Environmental Research Letters, 18, 024021, https://doi.org/10.1088/1748-9326/acb0e5, 2023.

He, Z., Gao, L., Liang, M., and Zeng, Z.-C.: A survey of methane point source emissions from coal mines in Shanxi province of China using AHSI on board Gaofen-5B, Atmos Meas Tech, 17, 2937–2956, https://doi.org/10.5194/amt-17-2937-2024, 2024.

Hong, X., Yang, K., and Liang, H.: Characterization of acidity and sulfate in dust obtained from the Wuda coal base, northern China: spatial distribution and pollution assessment, Environmental Science and Pollution Research, 28, 33219–33230, https://doi.org/10.1007/s11356-021-12897-8, 2021.

Irakulis-Loitxate, I., Guanter, L., Liu, Y.-N., Varon, D. J., Maasakkers, J. D., Zhang, Y., Chulakadabba, A., Wofsy, S. C., Thorpe, A. K., Duren, R. M., Frankenberg, C., Lyon, D. R., Hmiel, B., Cusworth, D. H., Zhang, Y., Segl, K., Gorroño, J., Sánchez-García, E., Sulprizio, M. P., Cao, K., Zhu, H., Liang, J., Li, X., Aben, I., and Jacob, D. J.: Satellite-based survey of extreme methane emissions in the Permian basin, Sci Adv, 7, eabf4507, https://doi.org/10.1126/sciadv.abf4507, 2024.

Jasansky, S., Lieber, M., Giljum, S., and Maus, V.: An open database on global coal and metal mine production, Sci Data, 10, 52, https://doi.org/10.1038/s41597-023-01965-y, 2023.

https://doi.org/10.5194/egusphere-2025-4610
Preprint. Discussion started: 17 March 2026

Kang, Y., Tian, P., Li, J., Wang, H., and Feng, K.: Methane mitigation potentials and related costs of China's coal mines, Fundamental Research, 4, 1688–1695, https://doi.org/10.1016/j.fmre.2023.09.012, 2024.
Khanna, N., Lin, J., Liu, X., and Wang, W.: An assessment of China's methane mitigation potential and costs and uncertainties through 2060, Nat Commun, 15, 9694, https://doi.org/10.1038/s41467-024-54038-y, 2024.
Langmuir, I.: THE ADSORPTION OF GASES ON PLANE SURFACES OF GLASS, MICA AND PLATINUM., J Am Chem Soc, 40, 1361–1403, https://doi.org/10.1021/ja02242a004, 1918.
Lauvaux, T., Giron, C., Mazzolini, M., d'Aspremont, A., Duren, R., Cusworth, D., Shindell, D., and Ciais, P.: Global assessment of oil and gas methane ultra-emitters, Science (1979), 375, 557–561, https://doi.org/10.1126/science.abj4351, 2022.
Li, F., Bai, S., Lin, K., Feng, C., Sun, S., Zhao, S., Wang, Z., Zhou, W., Zhou, C., and Zhang, Y.: Satellite-Based Surveys Reveal Substantial Methane Point-Source Emissions in Major Oil & Gas Basins of North America During 2022–2023, Journal of Geophysical Research: Atmospheres, 129, e2024JD040870, https://doi.org/10.1029/2024JD040870, 2024.
Lin, J., Zhang, J., Qiu, B., and Khanna, N.: Regional Production Shift and Increased Utilization Dampen Coal Mine Methane Emissions in China, https://doi.org/10.21203/rs.3.rs-6550772/v1, 11 May 2025.
Liu, G., Peng, S., Lin, X., Ciais, P., Li, X., Xi, Y., Lu, Z., Chang, J., Saunois, M., Wu, Y., Patra, P., Chandra, N., Zeng, H., and Piao, S.: Recent Slowdown of Anthropogenic Methane Emissions in China Driven by Stabilized Coal Production, Environ Sci Technol Lett, 8, 739–746, https://doi.org/10.1021/acs.estlett.1c00463, 2021.
Liu, Q., Teng, F., Nielsen, C. P., Zhang, Y., and Wu, L.: Large methane mitigation potential through prioritized closure of gas-rich coal mines, Nat Clim Chang, 14, 652–658, https://doi.org/10.1038/s41558-024-02004-3, 2024.
Lu, Y. Y., Zhang, H. D., Zhou, Z., Ge, Z. L., Chen, C. J., Hou, Y. D., and Ye, M. L.: Current Status and Effective Suggestions for Efficient Exploitation of Coalbed Methane in China: A Review, Energy & Fuels, 35, 9102–9123, https://doi.org/10.1021/acs.energyfuels.1c00460, 2021.
Miller, S. M., Michalak, A. M., Detmers, R. G., Hasekamp, O. P., Bruhwiler, L. M. P., and Schwietzke, S.: China's coal mine methane regulations have not curbed growing emissions, Nat Commun, 10, 303, https://doi.org/10.1038/s41467-018-07891-7, 2019.
Peng, S., Piao, S., Bousquet, P., Ciais, P., Li, B., Lin, X., Tao, S., Wang, Z., Zhang, Y., and Zhou, F.: Inventory of anthropogenic methane emissions in mainland China from 1980 to 2010, Atmos Chem Phys, 16, 14545–14562, https://doi.org/10.5194/acp-16-14545-2016, 2016.
Peng, S., Giron, C., Liu, G., d'Aspremont, A., Benoit, A., Lauvaux, T., Lin, X., de Almeida Rodrigues, H., Saunois, M., and Ciais, P.: High-resolution assessment of coal mining methane emissions by satellite in Shanxi, China, iScience, 26, 108375, https://doi.org/10.1016/j.isci.2023.108375, 2023.
Qin, K., Hu, W., He, Q., Lu, F., and Cohen, J. B.: Individual coal mine methane emissions constrained by eddy covariance measurements: low bias and missing sources, Atmos Chem Phys, 24, 3009–3028, https://doi.org/10.5194/acp-24-3009-2024, 2024.
Sadavarte, P., Pandey, S., Maasakkers, J. D., van der Gon, H. D., Houweling, S., and Aben, I.: A high-resolution gridded inventory of coal mine methane emissions for India and Australia, Elementa: Science of the Anthropocene, 10, 00056, https://doi.org/10.1525/elementa.2021.00056, 2022.
Saunois, M., Stavert, A. R., Poulter, B., Bousquet, P., Canadell, J. G., Jackson, R. B., Raymond, P. A., Dlugokencky, E. J., Houweling, S., Patra, P. K., Ciais, P., Arora, V. K., Bastviken, D., Bergamaschi, P., Blake, D. R., Brailsford, G., Bruhwiler, L., Carlson, K. M., Carrol, M., Castaldi, S., Chandra, N., Crevoisier, C., Crill, P. M., Covey, K., Curry, C. L., Etiope, G., Frankenberg, C., Gedney, N., Hegglin, M. I., Höglund-Isaksson, L., Hugelius, G., Ishizawa, M., Ito, A., Janssens-Maenhout, G., Jensen, K. M., Joos, F., Kleinen, T., Krummel, P. B., Langenfelds, R. L., Laruelle, G. G., Liu, L., Machida, T., Maksyutov, S., McDonald, K. C., McNorton, J., Miller, P. A., Melton, J. R., Morino, I., Müller, J., Murguia-Flores, F., Naik, V., Niwa, Y., Noce, S., O'Doherty, S., Parker, R. J., Peng, C., Peng, S., Peters, G. P., Prigent, C., Prinn, R., Ramonet, M., Regnier, P., Riley, W. J., Rosentreter, J. A., Segers, A., Simpson, I. J., Shi, H., Smith, S. J., Steele, L. P., Thornton, B. F., Tian, H., Tohjima, Y., Tubiello, F. N., Tsuruta, A., Viovy, N., Voulgarakis, A., Weber, T. S., van Weele, M., van der Werf, G. R., Weiss, R. F., Worthy, D., Wunch, D., Yin, Y., Yoshida, Y., Zhang, W., Zhang, Z., Zhao, Y., Zheng, B., Zhu, Q., Zhu, Q., and Zhuang, Q.: The Global Methane Budget 2000–2017, Earth Syst Sci Data, 12, 1561–1623, https://doi.org/10.5194/essd-12-1561-2020, 2020.
Scarpelli, T. R., Jacob, D. J., Grossman, S., Lu, X., Qu, Z., Sulprizio, M. P., Zhang, Y., Reuland, F., Gordon, D., and Worden, J. R.: Updated Global Fuel Exploitation Inventory (GFEI) for methane emissions from the oil, gas, and coal sectors: evaluation with inversions of atmospheric methane observations, Atmos Chem Phys, 22, 3235–3249, https://doi.org/10.5194/acp-22-3235-2022, 2022.

https://doi.org/10.5194/egusphere-2025-4610
Preprint. Discussion started: 17 March 2026

Scarpelli, T. R., Roy, E., Jacob, D. J., Sulprizio, M. P., Tate, R. D., and Cusworth, D. H.: Using new geospatial data and 2020 fossil fuel methane emissions for the Global Fuel Exploitation Inventory (GFEI) v3, Earth System Science Data Discussions, 2025, 1–23, https://doi.org/10.5194/essd-2024-552, 2025.

Schuit, B. J., Maasakkers, J. D., Bijl, P., Mahapatra, G., van den Berg, A.-W., Pandey, S., Lorente, A., Borsdorff, T., Houweling, S., Varon, D. J., McKeever, J., Jervis, D., Girard, M., Irakulis-Loitxate, I., Gorroño, J., Guanter, L., Cusworth, D. H., and Aben, I.: Automated detection and monitoring of methane super-emitters using satellite data, Atmos Chem Phys, 23, 9071–9098, https://doi.org/10.5194/acp-23-9071-2023, 2023.

Sheng, J., Song, S., Zhang, Y., Prinn, R. G., and Janssens-Maenhout, G.: Bottom-Up Estimates of Coal Mine Methane Emissions in China: A Gridded Inventory, Emission Factors, and Trends, Environ Sci Technol Lett, 6, 473–478, https://doi.org/10.1021/acs.estlett.9b00294, 2019.

Sherwin, E. D., Rutherford, J. S., Chen, Y., Aminfard, S., Kort, E. A., Jackson, R. B., and Brandt, A. R.: Single-blind validation of space-based point-source detection and quantification of onshore methane emissions, Sci Rep, 13, 3836, https://doi.org/10.1038/s41598-023-30761-2, 2023.

Sherwin, E. D., El Abbadi, S. H., Burdeau, P. M., Zhang, Z., Chen, Z., Rutherford, J. S., Chen, Y., and Brandt, A. R.: Single-blind test of nine methane-sensing satellite systems from three continents, Atmos Meas Tech, 17, 765–782, https://doi.org/10.5194/amt-17-765-2024, 2024.

Tan, M., Bian, Z., Dong, J., Hao, M., and Qu, J.: Comparing the variation and influencing factors of CO2 emission from subsidence waterbodies under different restoration modes in coal mining area, Environ Res, 237, 116936, https://doi.org/10.1016/j.envres.2023.116936, 2023.

Thompson, D. R., Leifer, I., Bovensmann, H., Eastwood, M., Fladeland, M., Frankenberg, C., Gerilowski, K., Green, R. O., Kratwurst, S., Krings, T., Luna, B., and Thorpe, A. K.: Real-time remote detection and measurement for airborne imaging spectroscopy: a case study with methane, Atmos Meas Tech, 8, 4383–4397, https://doi.org/10.5194/amt-8-4383-2015, 2015.

Tibrewal, K., Ciais, P., Saunois, M., Martinez, A., Lin, X., Thanwerdas, J., Deng, Z., Chevallier, F., Giron, C., Albergel, C., Tanaka, K., Patra, P., Tsuruta, A., Zheng, B., Belikov, D., Niwa, Y., Janardanan, R., Maksyutov, S., Segers, A., Tzompa-Sosa, Z. A., Bousquet, P., and Sciare, J.: Assessment of methane emissions from oil, gas and coal sectors across inventories and atmospheric inversions, Commun Earth Environ, 5, 26, https://doi.org/10.1038/s43247-023-01190-w, 2024.

Varon, D. J., Jacob, D. J., McKeever, J., Jervis, D., Durak, B. O. A., Xia, Y., and Huang, Y.: Quantifying methane point sources from fine-scale satellite observations of atmospheric methane plumes, Atmos Meas Tech, 11, 5673–5686, https://doi.org/10.5194/amt-11-5673-2018, 2018.

Wang, H., Zheng, B., Li, H., Zhang, Q., and He, K.: Targeting Ultra-Emitters for Effective Methane Mitigation in China's Coal Sector, ACS ES&T Air, 1, 734–742, https://doi.org/10.1021/acsestair.4c00069, 2024a.

Wang, T., Wu, F., Dickinson, D., and Zhao, W.: Energy price bubbles and extreme price movements: Evidence from China's coal market, Energy Econ, 129, 107253, https://doi.org/10.1016/j.eneco.2023.107253, 2024b.

Yang, Y., Dong, W., and Hui, J.: A Just Transition for Coal Regions: Learning from Two Coal Cities in Western China, 2024.

YUE Qun WANG Zheng, Z. G.: Preliminary estimation of methane emission and its distribution in China, GEOGRAPHICAL RESEARCH, 31, 1559–1570, https://doi.org/10.11821/yj2012090002, 2012.

Zhang, X., Zhu, T., Yi, N., Yuan, B., Li, C., Ye, Z., Zhu, Z., and Zhang, X.: Study on Characteristics and Model Prediction of Methane Emissions in Coal Mines: A Case Study of Shanxi Province, China, Atmosphere (Basel), 14, https://doi.org/10.3390/atmos14091422, 2023.

Zhang, Y., Fang, S., Chen, J., Lin, Y., Chen, Y., Liang, R., Jiang, K., Parker, R. J., Boesch, H., Steinbacher, M., Sheng, J.-X., Lu, X., Song, S., and Peng, S.: Observed changes in China's methane emissions linked to policy drivers, Proceedings of the National Academy of Sciences, 119, e2202742119, https://doi.org/10.1073/pnas.2202742119, 2022.